Error in the Finite Element Discretization of the Scalar Helmholtz Equation Over Electrically Large Regions

Andrew F. Peterson, *Member, IEEE,* and Richard J. Baca, *Student Member, IEEE*

Abstract—**Discretization error arising from a finite element solution of the scalar Helmholtz equation for open-region geometries is studied for the simple case of scattering from dielectric slabs. In electrically-large homogeneous regions, the primary source of error is found to be phase error that increases progressively in a direction away from the boundary where the excitation is coupled into the computational domain. The error can be reduced by using smaller cell sizes, employing higher order polynomial basis functions, or using a modified "scattered field" formulation that couples the excitation into the equation in a different manner.**

I. Introduction

ADVANCES in computer hardware, improvements in efficient sparse matrix technology, and the development of accurate radiation boundary conditions that mimic a semi-infinite space have prompted renewed interest in numerical solutions of the scalar and vector Helmholtz equations for electromagnetic scattering [1]–[13]. It is currently believed that electrically large or complex scatterer geometries can be analyzed more efficiently using these differential equation formulations than the traditional volume integral equation approaches [14]. Researchers have observed, however, that the accuracy of the differential equation formulations tends to degrade with increases in the electrical size of the region surrounding the scatterer [5], [8], [10]. Errors similar to standing waves were initially attributed to spurious reflections from the radiation boundaries, which sometimes must be located an appreciable distance from the scatterer to ensure accuracy [8], [15]–[16]. A recent study suggests that these errors are actually due to the discretization of the Helmholtz equation [5]. As an initial step in a systematic study of discretization error in electrically large regions, we examined the scattering of a plane wave from a simple dielectric slab [17]. Results of the study confirm that the discretization error grows in proportion to the electrical size of the region under consideration. Several ways of reducing the error are suggested.

Manuscript received April 12, 1991.

A. F. Peterson is with the School of Electrical Engineering, Georgia Institute of Technology, Atlanta, GA 30332-0250.

R. J. Baca is with the Department of Electrical and Computer Engineering, University of Illinois, Urbana, IL 61801.

IEEE Log Number 9101734.

II. Formulation

Consider a uniform plane wave having z-component of the form

$$E_z^{\text{inc}}(x) = E_0 e^{-jkx}, \tag{1}$$

normally incident on a dielectric slab of relative permittivity ϵ_r and relative permeability μ_r, located somewhere within the interval $a < x < b$. Following the usual definitions, E_z^{inc} represents the excitation in the absence of the scatterer and E_z^{tot} denotes the field produced in the presence of the scatterer. E_z^s is the difference defined so that

$$E_z^{\text{inc}}(x) + E_z^s(x) = E_z^{\text{tot}}(x). \tag{2}$$

The electric field can be obtained from the scalar Helmholtz equation

$$\frac{d}{dx}\left(\frac{1}{\mu_r}\frac{dE_z^{\text{tot}}}{dx}\right) + k^2\epsilon_r E_z^{\text{tot}} = 0, \qquad a < x < b, \tag{3}$$

subject to the boundary conditions

$$\frac{dE_z^s}{dx}\Big|_{x=a} = jkE_z^s, \tag{4}$$

$$\frac{dE_z^s}{dx}\Big|_{x=b} = -jkE_z^s. \tag{5}$$

To combine these constraints into a single equation amenable to discretization, (3) is multiplied by a testing function T and integrated over the computational domain to produce a "weak" form [8]. The boundary conditions and the incident field can be incorporated into the boundary term arising from integration-by-parts, to produce

$$\int_a^b \left\{\frac{1}{\mu_r}\frac{dT}{dx}\frac{dE_z^{\text{tot}}}{dx} - k^2\epsilon_r T E_z^{\text{tot}}\right\} dx + jkT(b)E_z^{\text{tot}}(b) + jkT(a)E_z^{\text{tot}}(a) = 2jkT(a)E_0 e^{-jka}. \tag{6}$$

Equation (6) represents a formulation in terms of the total field as the primary unknown. It is also possible to use the scattered field as the primary unknown, based on a slightly different derivation [4], [8] that produces

$$\int_a^b \left\{\frac{1}{\mu_r}\frac{dT}{dx}\frac{dE_z^s}{dx} - k^2\epsilon_r T E_z^s\right\} dx + jkT(b)E_z^s(b)$$

$$+ jk\,T(a)E_z^s(a) = \int_a^b T\left\{\frac{d}{dx}\left(\frac{1}{\mu_r}\frac{dE_z^{\text{inc}}}{dx}\right) + k^2\epsilon_r E_z^{\text{inc}}\right\} dx. \quad (7)$$

The left-hand sides of (6) and (7) are identical in form, and will discretize to produce the same matrix operator. However, the excitation is incorporated in a completely different manner in the right-hand sides of these equations.

We consider a traditional finite element discretization using Lagrangian basis or "shape" functions [18], and for brevity omit the details of the numerical implementation. For linear shape functions, the resulting matrix is tridiagonal. For quadratic shape functions, the matrix is pentadiagonal. The simple matrix structure facilitates the treatment of large systems representing electrically large geometries.

III. Results

Since exact solutions are readily available for the one-dimensional slab geometry, the error in the numerical solution as a function of position can be defined

$$\text{error}(x) = \frac{|\,E_z^{\text{tot}}(x)_{\text{exact}} - E_z^{\text{tot}}(x)_{\text{numerical}}\,|}{|\,E_z^{\text{tot}}(x)_{\text{exact}}\,|}. \quad (8)$$

Consider a plane wave incident on a slab having $\epsilon_r = 2$, $\mu_r = 1$, and a thickness of 1.0 λ, where λ denotes the wavelength in free space. The slab is located between $x = 0$ and $x = 1$ λ, with the boundaries of the computational domain located at $a = -20$ λ and $b = 21$ λ. For this geometry, the finite element representation extends over 41 wavelengths. We employ equal-sized cells throughout the free-space regions of the domain, with a slightly finer discretization with the slab to ensure a uniform representation with respect to the dielectric wavelength $\lambda_d = \lambda/(\epsilon_r\mu_r)^{1/2}$.

Fig. 1 depicts the error as a function of location for several different discretizations of (6), all of which employ linear basis and testing functions. With the exception of the 5 cells/λ curve, the general behavior of the error is to gradually increase from left to right throughout the domain. In the 5 cells/λ curve, the error oscillates in a sinusoidal fashion, reaching a maximum of approximately 2.0 at several locations throughout the region and returning to relatively small errors between these locations. As the cell density increases, the error grows at a much slower rate with distance into the computational domain.

Fig. 2 illustrates the error in the finite element solution of (7) using linear basis and testing functions, for the identical geometry used to produce Fig. 1. Although the error associated with the "scattered field formulation" appears to grow with distance at a similar rate as the error of the "total field formulation" depicted in Fig. 1, there are two main differences. First, the error in Fig. 2 begins to grow from the middle of the computational domain, at the location of the slab. Second, the error in Fig. 2 reaches a maximum of about 4.0, as compared to a maximum value of about 2.0 for Fig. 1.

The general trends depicted in Figs. 1 and 2 are consistent with progressive phase error that grows in a roughly linear

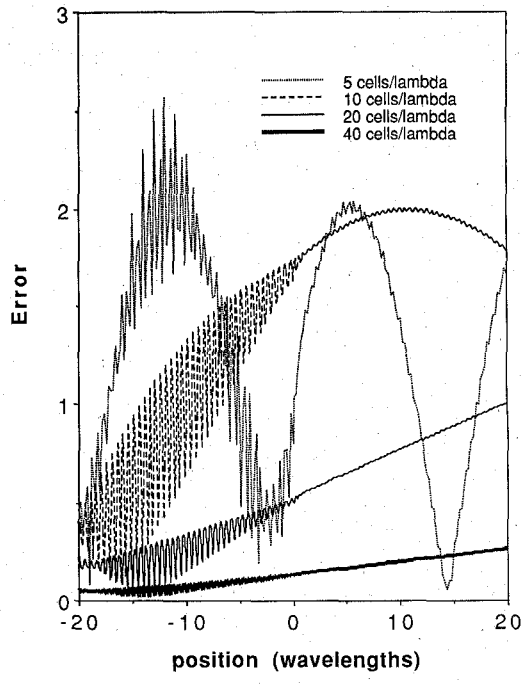

Fig. 1. Error (8) versus location for several discretizations of the "total" field formulation (6). A slab with $\epsilon_r = 2$ and $\mu_r = 1$ is located between $x = 0$ and $x = 1$ λ, where λ denotes the wavelength in the background medium. Computational domain is located between -20 and 21 λ. Numerical results were obtained using linear basis and testing functions.

fashion throughout the computational domain. The sinusoidal behavior illustrated in the 5 cells/λ curve of both figures can be attributed to phase error reaching 180 degrees at the location of the first maximum, and increasing to 360 degrees at the first minimum in the plot. (Assuming that the error is entirely in the phase of the total field, (8) achieves a theoretical peak value of 2.0 when the phase error reaches 180 degrees. To explain the error exhibited in Fig. 2, note that there are instances when the true total field is in phase opposition to the incident field. Under these circumstances, a phase error of 180 degrees in the scattered field can produce an error of 4.0 from (8)). The other curves shown in Figs. 1 and 2 illustrate a similar behavior, but with periods larger than the problem domain. Other test cases confirm that the growth rate of the phase error depends only on the cell density and not on the electrical size of the region [17]. Consequently, the maximum cumulative discretization error will be proportional to the electrical size of the domain under consideration.

The primary difference between the "total" and "scattered" field formulations appears to be the manner in which the incident field is incorporated into each equation. The total field formulation of (6) samples the incident field at the boundary of the computational domain (at $x = -20$ in Fig. 1), which is relatively far from the scatterer. In the scattered field formulation of (7), however, the incident field is sampled throughout the slab ($0 < x < 1$). In either formulation, the phase error grows in proportion to the distance away from the reference location.

Of course, the error illustrated in Figs. 1 and 2 is not entirely progressive phase error, and in inhomogeneous regions the behavior is usually far more complex [17]. This

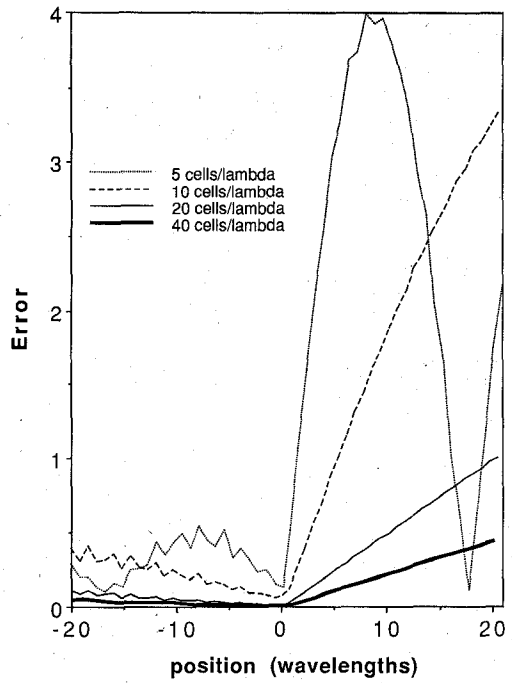

Fig. 2. Error (8) versus location for several discretizations of the "scattered" field formulation (7), applied to the identical slab geometry and computational domain used in Fig. 1. Numerical results were obtained using linear basis and testing functions.

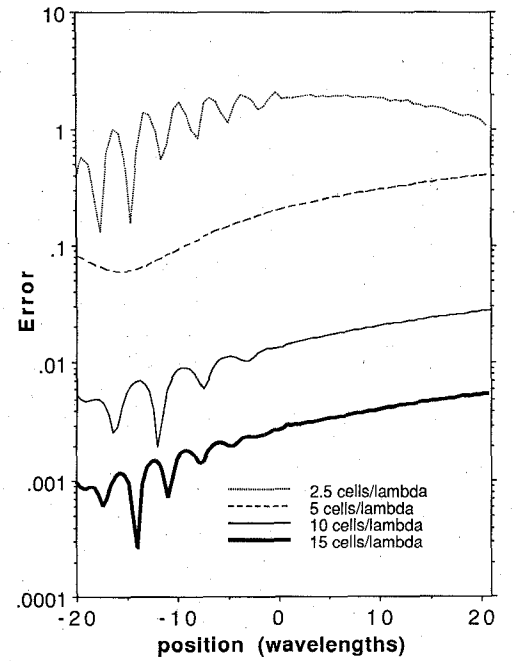

Fig. 3. Error (8) versus location for several discretizations of the "total" field formulation (6), applied to the identical slab geometry and computational domain used in Fig. 1. Numerical results were obtained using quadratic basis and testing functions.

particular test case exhibits extremely large errors; in fact, every result in these figures contains an unacceptable level of error. A possible remedy is the use of higher order basis and testing functions. The error arising from the total field formulation (6) using quadratic functions is illustrated in Fig. 3. Three quadratic basis functions overlap each cell in the domain, so the 2.5 cells/λ curve in Fig. 3 represents the same density of unknowns as the 5 cells/λ curve of Fig. 1. Although the accuracy attained with quadratic functions also appears to be ultimately limited by progressive phase error, the rate of growth of the error is significantly slower with the higher order algebraic functions. In addition, the absolute level of error is much smaller than that observed using the linear basis functions.

IV. Conclusion

This study has confirmed that discretization error in the finite element solution of the Helmholtz equation grows in proportion to the electrical size of the computational domain under consideration. Within an electrically large homogeneous region, the dominant error appears to be progressive phase error. As might be expected, a reduction in error is possible through the use of smaller cell sizes or the use of higher order polynomial basis and testing functions. Although the growth of phase error is similar for the "total" and "scattered" field formulations, the location of the phase reference is different. Since the scattered field formulation locates the phase reference within the scatterer, that formulation is likely to produce more accurate numerical solutions in the immediate vicinity of the scatterer than the total field formulation, especially if the scatterer is far from the boundaries of the computational domain.

References

[1] R. B. Wu and C. H. Chen, "Variational reaction formulation of scattering problem for anisotropic dielectric cylinders," *IEEE Trans. Antennas Propagat.*, vol. AP-34, no. 5, pp. 640-645, May 1986.

[2] K. K. Mei, "Unimoment method for electromagnetic wave scattering," *J. Electromagnetic Waves and Applicat.*, vol. 1, pp. 201-222, 1987.

[3] K. D. Paulsen, D. R. Lynch, and J. W. Strohbehn, "Three-dimensional finite, boundary, and hybrid element solutions of the Maxwell equations for lossy dielectric media," *IEEE Trans. Microwave Theory Tech.*, vol. 36, no 4, pp. 682-693, Apr. 1988.

[4] A. F. Peterson, "A comparison of integral, differential and hybrid methods for TE-wave scattering from inhomogeneous dielectric cylinders," *J. Electromagnetic Waves Applicat.*, vol. 3, pp. 87-106, 1989.

[5] L. W. Pearson, R. A. Whitaker, and L. J. Bahrmasel, "An exact radiation boundary condition for the finite element solution of electromagnetic scattering on an open domain," *IEEE Trans. Magn.*, vol. 25, pp. 3046-3048, July 1989.

[6] M. A. Morgan, Ed., *Finite Element and Finite Difference Methods in Electromagnetic Scattering.* New York: Elsevier, 1990.

[7] Z. Gong and A. W. Glisson, "A hybrid equation approach for the solution of electromagnetic scattering problems involving two-dimensional inhomogeneous dielectric cylinders," *IEEE Trans. Antennas Propagat.*, vol. 38, no. 1, pp. 60-68, Jan. 1990.

[8] A. F. Peterson and S. P. Castillo, "Differential equation methods for electromagnetic scattering from inhomogeneous cylinders," in *Radar Cross Sections of Complex Objects,* W. R. Stone, Ed. New York: IEEE Press, pp. 315-332, 1990.

[9] J. D'Angelo and I. D. Mayergoyz, "Finite element methods for the solution of RF radiation and scattering problems," *Electromagn.*, vol. 10, pp, 177-199, 1990.

[10] R. K. Gordon, "Radar scattering from bodies of revolution using an efficient partial differential equation algorithm," Ph.D. dissert., Univ. of Illinois, Urbana, 1990.

[11] X. Yuan, "Three-dimensional electromagnetic scattering from inhomogeneous objects by the hybrid moment and finite element method," *IEEE Trans. Microwave Theory Tech.*, vol. 38, no. 8, pp. 1053-1058, Aug. 1990.

[12] A. C. Cangellaris and R. Lee, "The bymoment method for two-dimensional electromagnetic scattering," *IEEE Trans. Antennas Propagat.*, vol. 38, no. 9, pp. 1429-1437, Sept. 1990.

[13] J. D. Collins, J. L. Volakis, and J. M. Jin, "A combined finite element-boundary integral formulation for solution of two-dimensional scattering problems via CGFFT," *IEEE Trans. Antennas Propagat.*, vol. 38, no. 11, pp. 1852–1858, Nov. 1990.

[14] A. F. Peterson, "Analysis of heterogeneous electromagnetic scatterers: Research progress of the past decade," *Proc. IEEE*, to appear, 1991.

[15] A. Bayliss and E. Turkel, "Radiation boundary conditions for wave-like equations," *Comm. Pure Appl. Math.*, vol. 33, pp. 707–725, 1980.

[16] A. F. Peterson, "Absorbing boundary conditions for the vector wave equation," *Microwave Opt. Tech. Letters*, vol. 1, pp. 62–64, Apr. 1988.

[17] R. J. Baca, "An investigation of the error in the finite element method applied to electromagnetics problems," M. S. thesis, Univ. of Illinois, Urbana, 1990.

[18] P. P. Silvester and R. L. Ferrari, *Finite Elements for Electrical Engineers, 2nd ed.* Cambridge: Cambridge Univ. Press, 1990.